IOP Publishing Journal of Physics A: Mathematical and Theoretical
J. Phys. A: Math. Theor. **52** (2019) 414002 (14pp) https://doi.org/10.1088/1751-8121/ab3f4e

Phase diagram of bipartite entanglement

Paolo Facchi[1,2,7], Giorgio Parisi[3], Saverio Pascazio[1,2], Antonello Scardicchio[4,5] and Kazuya Yuasa[6]

[1] Dipartimento di Fisica and MECENAS, Università di Bari, I-70126 Bari, Italy
[2] INFN, Sezione di Bari, I-70126 Bari, Italy
[3] Dipartimento di Fisica, Sapienza Università di Roma, INFN, Sezione di Roma 1, and CNR-Nanotec, Rome Unit, I-00185 Rome, Italy
[4] The Abdus Salam ICTP, I-34151 Trieste, Italy
[5] INFN, Sezione di Trieste, I-34127 Trieste, Italy
[6] Department of Physics, Waseda University, Tokyo 169-8555, Japan

E-mail: paolo.facchi@ba.infn.it

Received 10 April 2019, revised 19 July 2019
Accepted for publication 29 August 2019
Published 18 September 2019

Abstract

We investigate the features of the entanglement spectrum (distribution of the eigenvalues of the reduced density matrix) of a large quantum system in a pure state. We consider all Rényi entropies and recover purity and von Neumann entropy as particular cases. We construct the phase diagram of the theory and unveil the presence of two critical lines.

Keywords: entanglement, phase transitions, random matrix theory

(Some figures may appear in colour only in the online journal)

1. Introduction

The notion of entanglement is central in the emerging fields of quantum technologies and quantum applications [1]. Entanglement is a genuine non-classical feature of quantum states [2] and characterizes the nonclassical correlations among the different components of a quantum system. It can be measured in terms of different quantities, such as purity and von Neumann entropy [3–5].

For large quantum systems, the distribution of bipartite entanglement is pivotal to understand the features of the many-body wave function. Interestingly, random pure states play a crucial role in this context: they are characterized by a large entanglement and display a number of interesting features. The first studies on this subject date back to forty years ago and focused on the average purity of a bipartite system, that turns out to be almost minimal for randomly sampled states [6]. These findings were extended to the average von Neumann

[7] Author to whom any correspondence should be addressed.

entropy [7–10] and to higher moments [11], and are essentially a consequence of the concentration of measure for the so-called entanglement spectrum (the eigenvalues of the reduced density matrix) [12].

The typical entanglement spectrum was eventually determined [13–15] and displayed the presence of phase transitions. These studies focused on the purity, and were soon extended to different Rényi entropies [16, 17] and eventually to the von Neumann entropy [18]. It is in fact somewhat surprising that a number of interesting results can be obtained analytically, probably because they hinge on the Coulomb gas method [19, 20] and the ensuing saddle point equations [21–24].

In the approach proposed in [13] one 'biases' the amount of entanglement across the (given) bipartition and studies typicality constrained at such entanglement. This yields a family of entanglement spectra that depend on the adopted measure of entanglement and whose features are of great interest. One unveils the presence of two phase transitions, as the entanglement between the two partitions is changed. One of them is due to the 'evaporation' of the largest eigenvalue, which splits off from the continuous distribution of eigenvalues [25, 26], while the other one to the vanishing of the smallest eigenvalue and to the squeezing of the distribution against the hard wall at zero (pushed-to-pulled transition) [27–31].

In this Article we shall scrutinize the features of the two phase transitions for all Rényi entropies. We shall find that the entropies for generic $q > 1$, although very interesting [16, 17], display no qualitative differences with respect to the case of purity, $q = 2$ [13]: the order of the phase transitions is preserved and the distributions of the eigenvalues are expected to be slightly deformed; also, in all cases, a single eigenvalue evaporates out of the continuum. On the other hand, as anticipated in [18], both phase transitions for the von Neumann entropy are smoother than for all Rényi entropies, and in particular one of them becomes continuous when the other one is of first order.

This work is organized as follows. We define the problem and set up our notation in section 2. The *entangled*, *typical* and *separable phases* are analyzed in sections 3–5, respectively. The phase diagram is drawn in section 6. We conclude in section 7.

2. Setting up the problem

Let the total quantum system be composed of two balanced parts A and $\bar{A}$, the total Hilbert space being $\mathcal{H} = \mathcal{H}_A \otimes \mathcal{H}_{\bar{A}}$, with $\dim\mathcal{H}_A = \dim\mathcal{H}_{\bar{A}} = N$. Let us also assume that the total state is pure, $|\psi\rangle$, so that the density matrix of A reads

$$\varrho_A = \mathrm{tr}_{\bar{A}}|\psi\rangle\langle\psi|, \tag{1}$$

with $\varrho_A \geqslant 0$ and $\mathrm{tr}\varrho_A = 1$. We quantify the bipartite entanglement across the bipartition by the Rényi entropy of ϱ_A,

$$S_q(\vec{\lambda}) = -\frac{1}{q-1}\ln\left(\sum_{k=1}^{N}\lambda_k^q\right), \tag{2}$$

where $\vec{\lambda} = (\lambda_1, \ldots, \lambda_N) \in \Delta_{N-1}$ are the eigenvalues of ϱ_A, and $\Delta_{N-1} = \{\lambda_k \geqslant 0, \sum_k \lambda_k = 1\}$.

The Rényi entropy ranges between $0 \leqslant S_q \leqslant \ln N$, where the minimum is attained by separable states and the maximum by maximally entangled states. Note that the Rényi entropy reduces to the von Neumann entropy $S_1 = -\sum_k \lambda_k \ln\lambda_k$ in the limit $q \to 1$.

We are interested in the typical entanglement spectrum. For random states $|\psi\rangle$, uniformly sampled on the unit sphere $\langle\psi|\psi\rangle = 1$, the eigenvalues $\vec{\lambda}$ are distributed according to the (Haar) joint probability density function [32–34]

$$p_N(\vec{\lambda}) = C_N \prod_{1\leqslant j<k\leqslant N} (\lambda_j - \lambda_k)^2, \tag{3}$$

C_N being a normalization factor. For large N, the distribution p_N concentrates around a typical value $\vec{\lambda}$, that maximizes p_N [12], and the spectrum of ϱ_A follows a Marčenko–Pastur law [35] with support $[0, 4/N]$ [13].

We shall ask here how the entanglement spectrum looks like in a system with a given value of the entropy S_q, fixing the bipartite entanglement. This is nothing but a constrained maximization problem. Let

$$u = \ln N - S_q(\vec{\lambda}) = \frac{1}{q-1} \ln \left(\frac{1}{N} \sum_k (N\lambda_k)^q \right), \tag{4}$$

which quantifies the deviation of the entropy S_q from its maximum value $\ln N$. Then, given a value $u \in [0, \ln N]$, we seek $\vec{\lambda}_{\max}$ such that

$$p_N(\vec{\lambda}_{\max}) = \max \left\{ p_N(\vec{\lambda}) \,:\, \vec{\lambda} \in \Delta_{N-1},\, S_q(\vec{\lambda}) = \ln N - u \right\}. \tag{5}$$

By introducing two Lagrange multipliers ξ and β, that constrain the eigenvalue normalization and the deviation u of the entropy from its maximum $\ln N$, respectively, the problem is translated into the (unconstrained) minimization of the potential

$$\begin{aligned} V(\vec{\lambda}, \xi, \beta) = &-\frac{2}{N^2} \sum_{j<k} \ln|\lambda_j - \lambda_k| + \xi \left(\sum_k \lambda_k - 1 \right) \\ &+ \beta \left[\frac{1}{q-1} \ln \left(\frac{1}{N} \sum_k (N\lambda_k)^q - \sum_k \lambda_k + 1 \right) - u \right] \end{aligned} \tag{6}$$

with respect to $\vec{\lambda}$, ξ, and β. Note that we have added two terms in the logarithm that expresses the constraint on the entropy; otherwise, the expression is not well defined for $q \to 1$ before imposing the other constraint on the eigenvalue normalization.

This problem is equivalent to the statistical mechanics of points on the simplex Δ_{N-1} with partition function [13]

$$Z_N = \int_{\Delta_{N-1}} \mathrm{e}^{-\beta N^2 E(\vec{\lambda})} p_N(\vec{\lambda})\, \mathrm{d}^N\lambda, \tag{7}$$

where $E(\vec{\lambda}) = \ln N - S_q(\vec{\lambda})$ is the 'energy density' and β the inverse 'temperature'. As $N \to \infty$, the partition function is given by the maximum of the integrand, i.e. the minimum of the potential (6). Highly entangled states are obtained for large values of β, maximally entangled states for $\beta = +\infty$, and typical states for $\beta = 0$.

The saddle-point equations read

$$\frac{\partial V}{\partial \lambda_j} = \frac{2}{N} \sum_{k\neq j} \frac{1}{N\lambda_k - N\lambda_j} + \frac{\beta}{q-1} \frac{q(N\lambda_j)^{q-1} - 1}{\frac{1}{N}\sum_k (N\lambda_k)^q - \frac{1}{N}\sum_k N\lambda_k + 1} + \xi = 0, \tag{8}$$

$$\frac{\partial V}{\partial \beta} = \frac{1}{q-1} \ln \left(\frac{1}{N} \sum_k (N\lambda_k)^q - \frac{1}{N} \sum_k N\lambda_k + 1 \right) - u = 0, \tag{9}$$

$$\frac{\partial V}{\partial \xi} = \frac{1}{N}\sum_k N\lambda_k - 1 = 0. \tag{10}$$

When all the eigenvalues λ_k are of order $O(1/N)$, we introduce the empirical eigenvalue distribution

$$\sigma(\lambda) = \frac{1}{N}\sum_k \delta(\lambda - N\lambda_k), \tag{11}$$

with

$$\int \mathrm{d}\lambda\, \sigma(\lambda) = 1, \tag{12}$$

and equations (8)–(10) read

$$2 \fint \mathrm{d}\lambda' \, \frac{\sigma(\lambda')}{\lambda' - \lambda} + \beta \mathrm{e}^{-(q-1)u} \frac{q\lambda^{q-1} - 1}{q-1} + \xi = 0, \tag{13}$$

$$\int \mathrm{d}\lambda\, \sigma(\lambda)\lambda = 1, \tag{14}$$

$$u = \frac{1}{q-1} \ln\left(\int \mathrm{d}\lambda\, \sigma(\lambda)\lambda^q \right), \tag{15}$$

with $\lambda = N\lambda_j$, and $\fint$ denoting the Cauchy principal value.

The above expressions are suitable to the limit $N \to +\infty$. The integral equation (13) admits a solution $\sigma(\lambda)$ that lies within a compact support

$$\lambda \in [a, b], \qquad \text{with} \quad a \geqslant 0, \tag{16}$$

and can be obtained via a theorem by Tricomi [36]. Let us change the variable from λ to $x \in [-1, 1]$ by

$$\lambda = \delta(x + \alpha), \qquad \delta = \frac{b-a}{2}, \qquad \alpha = \frac{b+a}{b-a} = 1 + \frac{a}{\delta}, \tag{17}$$

so that the distribution $\phi(x)$ of x is related to $\sigma(\lambda)$ through

$$\sigma(\lambda) = \frac{1}{\delta}\phi(x). \tag{18}$$

In terms of these quantities, the equations in (13) and (14) read

$$\frac{1}{\pi} \fint_{-1}^{1} \mathrm{d}y \, \frac{\phi(y)}{y - x} = -\frac{\delta}{2\pi} \left(\beta \mathrm{e}^{-(q-1)u} \frac{q\delta^{q-1}(x+\alpha)^{q-1} - 1}{q-1} + \xi \right), \tag{19}$$

$$\int_{-1}^{1} \mathrm{d}x\, \phi(x) x = \frac{1}{\delta} - \alpha. \tag{20}$$

Their solution is given by

$$\phi(x) = \frac{1}{\pi\sqrt{1-x^2}} [1 - Ax + Bh(x, \alpha)], \tag{21}$$

where

$$A = \frac{\delta}{2}\left(\beta \mathrm{e}^{-(q-1)u}\frac{q\delta^{q-1}-1}{q-1} + \xi\right), \qquad B = \frac{1}{2}\beta q \delta^q \mathrm{e}^{-(q-1)u}, \tag{22}$$

$$h(x,\alpha) = \frac{1}{\pi}\fint_{-1}^{1} \mathrm{d}y\, \frac{\sqrt{1-y^2}}{y-x}\frac{(y+\alpha)^{q-1}-1}{q-1}. \tag{23}$$

The last equation (15) reads

$$u = \frac{1}{q-1}\ln\left(\delta^q \int_{-1}^{1} \mathrm{d}x\, \phi(x)(x+\alpha)^q\right). \tag{24}$$

We are now ready to investigate the behavior of the entanglement spectrum as q and u are varied. Remember that, from equation (4), u can be viewed as the opposite of the entanglement between the two bipartitions of the total system. See equations (1) and (2).

3. Entangled phase ($\alpha > 1$, small u)

Large values of bipartite entanglement correspond to small values of u. They are obtained for low temperatures (large β in equation (7)). The limit of the empirical measure is compactly supported in $\lambda \in [a,b]$, with

$$0 < a < b, \qquad \Rightarrow \qquad \alpha > 1. \tag{25}$$

The values of the extremes of the support of the distribution, a and b, and thus δ and α in (17), can be determined by imposing the constraint (20) and the conditions of regularity at both ends of the distribution,

$$\phi(-1) = 0, \qquad \text{and} \quad \phi(1) = 0, \tag{26}$$

which yield

$$-\frac{1}{2}A - Bg(\alpha) = \frac{1}{\delta} - \alpha, \tag{27}$$

$$1 - A + Bh(1,\alpha) = 0, \tag{28}$$

$$1 + A + Bh(-1,\alpha) = 0, \tag{29}$$

with

$$g(\alpha) = \frac{1}{\pi}\int_{-1}^{1} \mathrm{d}y\, \sqrt{1-y^2}\frac{(y+\alpha)^{q-1}-1}{q-1}. \tag{30}$$

One gets

$$A = -\frac{h(1,\alpha) - h(-1,\alpha)}{h(1,\alpha) + h(-1,\alpha)}, \tag{31}$$

$$B = -\frac{2}{h(1,\alpha) + h(-1,\alpha)}, \tag{32}$$

$$\delta = \left(\alpha - \frac{1}{2}A - Bg(\alpha)\right)^{-1}, \tag{33}$$

for $\alpha > 1$. These expressions are valid for what we shall call the 'entangled' phase. There are two interesting particular cases:

- **von Neumann entropy, $q \to 1$:** In this limit, we have

$$A = (\alpha + \sqrt{\alpha^2 - 1}) \ln[2(\alpha - \sqrt{\alpha^2 - 1})], \tag{34}$$

$$B = \alpha + \sqrt{\alpha^2 - 1}, \tag{35}$$

$$\delta = \frac{4}{3\alpha + \sqrt{\alpha^2 - 1}}, \tag{36}$$

  for $\alpha > 1$. Finally, u is given by [18]

$$u = \ln\left(1 - \frac{1}{2\beta}\right) + \frac{1}{\beta}, \tag{37}$$

  where β is obtained from the definition of B in (22):

$$\beta = \frac{1}{2}(\alpha + \sqrt{\alpha^2 - 1})(3\alpha + \sqrt{\alpha^2 - 1}). \tag{38}$$

  The function $\beta(\alpha)$ is strictly increasing for $\alpha > 1$, with $\beta(1) = 3/2$ and $\beta \to \infty$ as $\alpha \to \infty$, while $u(\beta)$ is strictly decreasing for $\beta > 3/2$ with $u(3/2) = 2/3 + \ln(2/3)$ and $u \to 0$ as $\beta \to \infty$. Therefore equation (37) can be inverted to get α as a function of u. These results are consistent with those obtained in [18] for the von Neumann entropy.
- **purity, $q = 2$:** In this case, already considered in [13, 14], we have

$$A = -2(\alpha - 1), \qquad B = 2, \qquad \delta = \alpha^{-1} \qquad (\alpha > 1), \tag{39}$$

  and

$$\phi(x) = \frac{2}{\pi}\sqrt{1 - x^2}, \quad \sigma(\lambda) = \frac{2\alpha^2}{\pi}\sqrt{\frac{1}{\alpha^2} - (\lambda - 1)^2}, \tag{40}$$

  with

$$\alpha = \frac{1}{2}(\mathrm{e}^u - 1)^{-1/2}. \tag{41}$$

As u (and thus the temperature) is increased, and $\alpha \downarrow 1$ accordingly, the left end a of the distribution $\sigma(\lambda)$ of the eigenvalues touches the boundary at $\lambda = 0$, that is $a = 0$ ($\alpha = 1$), and the system reaches the first phase-transition line $u_C(q)$, where

$$A_C(q) = -1 - \frac{1}{q - 1}\left(1 - \frac{\sqrt{\pi}\Gamma(q + 1)}{2^{q-1}\Gamma(q - 1/2)}\right), \tag{42}$$

$$B_C(q) = \frac{\sqrt{\pi}\Gamma(q + 1)}{2^{q-1}\Gamma(q - 1/2)}, \tag{43}$$

$$\delta_C(q) = \frac{2(q+1)}{3q}, \tag{44}$$

at $\alpha = 1$. The explicit expression of u along the critical line,

$$u_C(q) = \frac{1}{q-1} \ln \left[\left(\frac{4(q+1)}{3q} \right)^q \frac{\Gamma(q+3/2)}{\sqrt{\pi}\Gamma(q+2)} \right], \tag{45}$$

is in accord with [16, 17], and is obtained by evaluating at $\delta = \delta_C(q)$ the expression of u derived in (50) in the next section. The (whole) phase diagram will be shown in figure 5.

4. Typical phase ($\alpha = 1$, intermediate u)

We keep increasing u (and temperature), and thus lowering entanglement, beyond the first critical line $u_C(q)$. In this regime,

$$0 = a < b, \qquad \Rightarrow \qquad \alpha = 1, \tag{46}$$

and we impose only the constraint (20) and the condition

$$\phi(1) = 0, \tag{47}$$

namely the conditions (27) and (28). We get

$$A = 1 - \frac{2/\delta - 1}{q-1} \left(q + 1 - \frac{\sqrt{\pi}\Gamma(q+2)}{2^q \Gamma(q+1/2)} \right), \tag{48}$$

$$B = (2/\delta - 1) \frac{\sqrt{\pi}\Gamma(q+2)}{2^q \Gamma(q+1/2)}. \tag{49}$$

An explicit expression of u in this phase is available as a function of δ and q,

$$u = \frac{1}{q-1} \ln \left[\left(\frac{q+1}{\delta} - \frac{q-1}{2} \right) \frac{(2\delta)^q \Gamma(q+1/2)}{\sqrt{\pi}\Gamma(q+2)} \right]. \tag{50}$$

The first critical $u_C(q)$ line is reached at $\delta = \delta_C(q)$ in (44). A second critical line $u_E(q)$ is reached at

$$\delta_E(q) = 2, \qquad (\beta_E = 0), \tag{51}$$

where, in accord with [16, 17],

$$u_E(q) = \frac{1}{q-1} \ln \left(\frac{2^{2q}\Gamma(q+1/2)}{\sqrt{\pi}\Gamma(q+2)} \right), \tag{52}$$

and

$$\phi_{\mathrm{MP}}(x) = \frac{1}{\pi} \sqrt{\frac{1-x}{1+x}}, \qquad \sigma_{\mathrm{MP}}(\lambda) = \frac{1}{2\pi} \sqrt{\frac{4-\lambda}{\lambda}}. \tag{53}$$

This is the Marčenko–Pastur law, the distribution of typical states.

5. Separable phase (large *u*)

We can reach lower values of entanglement, towards the separable states, by increasing u above the second critical line $u_E(q)$. This corresponds to negative temperatures $\beta < 0$ of the statistical-mechanics model.

In the separable phase, one eigenvalue $\lambda_1 = \mu = O(1)$ while the others $\lambda_k = O(1/N)$ ($k \geqslant 2$). In this case, the saddle point equations in (8)–(10) reduce, for large N, to

$$\frac{2}{N^2} \sum_{k\geqslant 2, k\neq j} \frac{1}{\lambda_k - \lambda_j} + \xi = 0 \qquad (j \geqslant 2), \tag{54}$$

$$\sum_{k\geqslant 2} \lambda_k = 1 - \mu, \qquad \xi = -\beta \frac{q(N\mu)^{q-1} - 1}{(q-1)N^{q-1}\mu^q}, \tag{55}$$

$$u = \frac{1}{q-1} \ln(N^{q-1}\mu^q - \mu + 1). \tag{56}$$

By introducing the empirical distribution

$$\tilde{\sigma}(\lambda) = \frac{1}{N-1} \sum_{k\geqslant 2} \delta\left(\lambda - \frac{N-1}{1-\mu}\lambda_k\right), \tag{57}$$

these equations become

$$2 \fint \mathrm{d}\lambda' \, \frac{\tilde{\sigma}(\lambda')}{\lambda' - \lambda} + \xi(1-\mu) = 0, \tag{58}$$

$$\int \mathrm{d}\lambda \, \tilde{\sigma}(\lambda) = 1, \qquad \int \mathrm{d}\lambda \, \tilde{\sigma}(\lambda)\lambda = 1, \tag{59}$$

with

$$u = \frac{1}{q-1} \ln(N^{q-1}\mu^q - \mu + 1), \tag{60}$$

$$\xi = -\beta \frac{q(N\mu)^{q-1} - 1}{(q-1)N^{q-1}\mu^q}, \tag{61}$$

and $\lambda = (N-1)\lambda_j/(1-\mu)$. The set of equations (58) and (59) is formally equivalent to (13) and (14) with $\beta \to 0$ and $\xi \to \xi(1-\mu)$. Therefore, the solution is obtained by translating the result for $\beta = 0$ in the previous subsection,

$$\tilde{\sigma}_{\mathrm{MP}}(\lambda) = \frac{1}{2\pi} \sqrt{\frac{4-\lambda}{\lambda}}, \qquad \xi = -\beta \frac{q(N\mu)^{q-1} - 1}{(q-1)N^{q-1}\mu^q} = \frac{1}{1-\mu}. \tag{62}$$

6. The phase diagram

Some entanglement spectra are displayed in figures 1–4. The spectra for $q = 2$ and $q = 1$ were shown in [14] and [18], respectively. The spectra for a generic $q \neq 1, 2$ are novel and we show an example in figure 3. The deformations of the spectra for different q are very interesting and are easily understood by observing that large values of q tend to attribute more 'weight' to

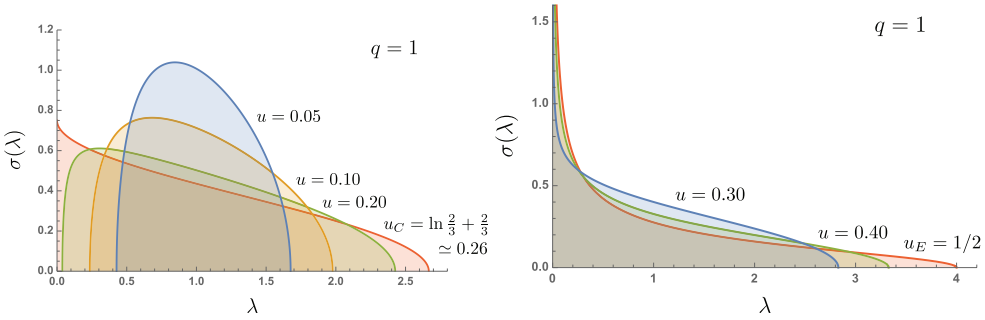

Figure 1. Entanglement spectra $\sigma(\lambda)$ at $q = 1$ for various values of the von Neumann entropy $S_1 = \ln N - u$: entanglement decreases as u increases. (a) Entangled phase: $0 \leqslant u \leqslant u_C(1) = \ln(2/3) + 2/3$, (b) typical phase: $u_C(1) \leqslant u \leqslant u_E(1) = 1/2$. Both $u_C(1)$ and $u_E(1)$ are critical values belonging to the critical lines $u_C(q)$ and $u_E(q)$, see figure 5.

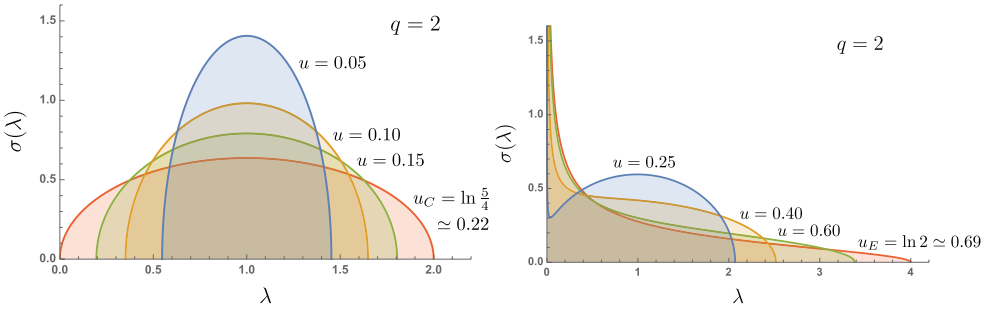

Figure 2. Entanglement spectra $\sigma(\lambda)$ at $q = 2$ for various values of (the logarithm of) the purity $S_2 = \ln N - u$: entanglement decreases as u increases. (a) Entangled phase: $0 \leqslant u \leqslant u_C(2) = \ln(5/4)$, (b) typical phase: $u_C(2) \leqslant u \leqslant u_E(2) = \ln 2$. Both $u_C(2)$ and $u_E(2)$ are critical values belonging to the critical lines $u_C(q)$ and $u_E(q)$, see figure 5.

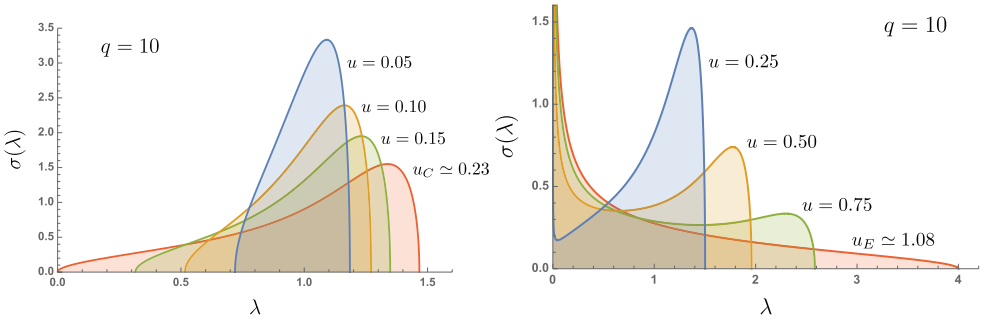

Figure 3. Entanglement spectra $\sigma(\lambda)$ at $q = 10$ for various values of the Rényi entropy $S_{10} = \ln N - u$: entanglement decreases as u increases. (a) Entangled phase: $0 \leqslant u \leqslant u_C(10) \simeq 0.23$, (b) typical phase: $u_C(10) \leqslant u \leqslant u_E(10) \simeq 1.08$. Both $u_C(10)$ and $u_E(10)$ are critical values belonging to the critical lines $u_C(q)$ and $u_E(q)$, see figure 5.

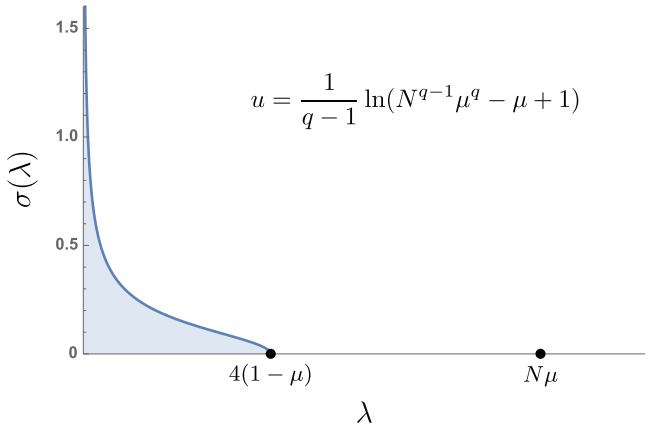

Figure 4. Entanglement spectra $\sigma(\lambda)$ in the separable phase $u_E(q) < u \leqslant \ln N$. One eigenvalue has evaporated from the spectrum sea, which has a Marčenko–Pastur distribution.

large eigenvalues. For any q, at $u = u_E(q)$, one eigenvalue evaporates from the spectrum sea $O(1/N)$ and becomes $O(1)$. See figure 4.

As anticipated, as q and u are varied, one encounters two critical lines. See figure 5. Starting from small values of u (large entanglement $S_q = \ln N - u$ across the bipartition), one encounters a first phase transition at $u = u_C(q)$. This first critical line separates an 'entangled' phase (red in the figure), present for $0 < u < u_C$, from a 'typical' phase (blue in the figure).

In the entangled phase the entanglement spectrum is a (deformed) semicircle around $1/N$. Notice that as $u \downarrow 0$ the semicircle degenerates into a Dirac delta, corresponding to maximally entangled states.

Across the critical line $u = u_C(q)$ the so-called pushed-to-pulled transition takes place. We call it the 'concentration' line, here the gap closes and the entanglement spectrum touches the boundary $\lambda = 0$, so that the left endpoint $a = 0$. Above this critical line a sharp concentration of eigenvalues near zero is formed with the development of a sharp (integrable) spike. Observe that $u_C(q) \to \ln(4/3)$ as $q \to \infty$. Along the concentration line $u = u_C(q)$ the phase transition is third order [14], *except* at $q = 1$, where it becomes fourth order [18].

As u increases, for $u_C < u < u_E$, one finds the typical phase. Eventually, one reaches the second critical line $u = u_E(q)$, which separates the typical phase from a 'separable' phase (green in the figure), present for $u_E < u < \ln N$.

The value $u = u_E(q)$ is characterized by the onset of evaporation of the largest eigenvalue. For $u = u_E(q)$ the distribution is Marčenko–Pastur. Observe that $u_E(q) \to 2\ln 2$ as $q \to \infty$, and $u = \ln N$ for genuinely separable states. Along the evaporation line $u = u_E(q)$ the phase transition is first order [14], *except* at $q = 1$, where it becomes second order [18]. Interestingly, at $q = 1$ the phase transitions are softer.

All phase transitions are detected by a change in the entanglement spectrum. This is reflected in a sharp variation of the relative volume of the manifolds with constant entanglement (isoentropic manifolds) [14].

We observe that states above the first asymptote, at $q = 2\ln 2$, always have a significant separable component $O(1)$, independently of the value of q, and therefore of the Rényi entropy used to measure entanglement. We call them 'entropy-independent separable states' (EISS). States below the parallel line tangent to the minimum of $u_C(q)$ are significantly entangled, independently of the value of q, and therefore of the particular Rényi entropy. We call them

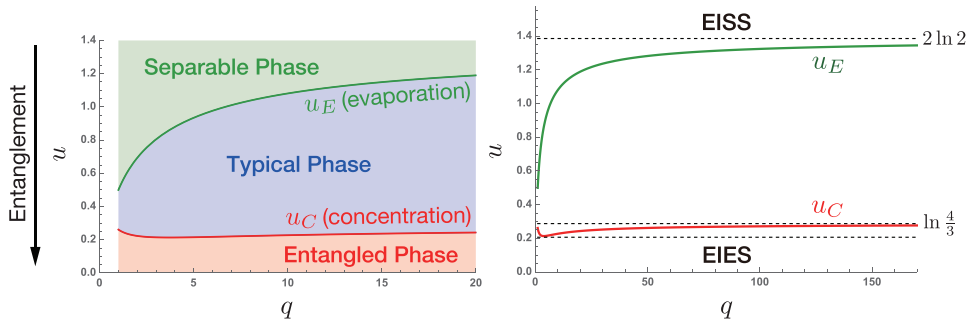

Figure 5. Left. Phase diagram of the entanglement spectrum, (q,u)-plane. The entanglement $S_q = \ln N - u$ decreases as u increases. The entangled phase (red) is for $0 < u < u_C$: the eigenvalue distribution is a (deformed) semicircle around $1/N$; as $u \downarrow 0$ the semicircle degenerates into a Dirac delta and the state is maximally entangled. The critical line $u = u_C(q)$ is the 'concentration' line (pushed-to-pulled transition) where the gap closes, the left endpoint of the entanglement spectrum touches the boundary $\lambda = 0$ and the entanglement spectrum starts developing a sharp concentration of eigenvalues near zero; $u_C(q) \to \ln(4/3)$ as $q \to \infty$. The typical phase (blue) is for $u_C < u < u_E$: the critical line $u = u_E(q)$ is the 'evaporation' line, corresponding to typical states. The largest eigenvalue evaporates from the spectrum sea, characterized by a Marčenko–Pastur distribution; $u_E(q) \to 2\ln 2$ as $q \to \infty$. The separable phase (green) is for $u_E < u < \ln N$: the line $u = \ln N$ (not shown) corresponds to separable states. Right. Same phase diagram for a wider range of q. Observe that $u_C(q)$ has a minimum $u_C \simeq 0.214$ at $q \simeq 3.733$. States EIES (entropy-independent entangled states) below the lowest dashed line are entangled independently of the adopted entropy measure (namely, the value of q). States EISS (entropy-independent separable states) above the dashed asymptote have a significant ($O(1)$) separable component independently of the adopted entropy measure (namely, the value of q).

'entropy-independent entangled states' (EIES). Further investigation is needed to understand what EISS and EIES are and if they have some sort of characterization.

7. Conclusions and perspectives

We have determined the phase diagram of the entanglement spectrum for a bipartite quantum system. The analysis hinges upon saddle point equations and a Coulomb gas method. It is valid in the limit of large quantum systems. The present analysis basically completes the characterization of typical bipartite entanglement for balanced bipartitions and Rényi entropies of order $q \geqslant 1$.

There are (at least) three possible extensions of the present analysis: all are very interesting from the fundamental point of view and possibly in terms of applications. These analyses will be postponed to sequel papers, but we would like to briefly comment on them.

(i) Our analysis and the phase transitions pertain to the case $q \geqslant 1$. It would be interesting to understand if the general picture outlined in this Article remains valid for $0 \leqslant q < 1$.

(ii) We considered a balanced bipartition $\dim\mathcal{H}_A = \dim\mathcal{H}_{\bar{A}}$. Define

$$\Delta = \frac{\dim\mathcal{H}_A - \dim\mathcal{H}_{\bar{A}}}{\dim\mathcal{H}_A}, \tag{63}$$

for which the first moments of purity, but not the full distributions, are known [13]. This is an additional freedom. The diagram in figure 5 corresponds to the section at $\Delta = 0$ of a three-dimensional phase diagram.

(iii) We focused on bipartite entanglement. *Multipartite* entanglement is much more difficult to study. One possible strategy consists in looking at the distribution of bipartite entanglement when the bipartition is varied [37, 38]. This problem is more difficult, and no complete characterization exists, although a number of interesting ideas have been proposed, in particular for small subsystems [39–44]. One of the main roadblocks seems to be the presence of frustration [45], which makes the analysis (and the numerics) more involved. A thorough understanding of multipartite entanglement is however crucial, also in view of possible quantum applications [46].

Acknowledgments

We thank Beppe Marmo for interesting discussions. PF and SP are partially supported by Istituto Nazionale di Fisica Nucleare (INFN) through the project 'QUANTUM'. PF is partially supported by the Italian National Group of Mathematical Physics (GNFM-INdAM). KY is partially supported by the Top Global University Project from the Ministry of Education, Culture, Sports, Science and Technology (MEXT), Japan, by the Grants-in-Aid for Scientific Research (C) (No. 18K03470) and for Fostering Joint International Research (B) (No. 18KK0073) both from the Japan Society for the Promotion of Science (JSPS), and by the Waseda University Grant for Special Research Projects (No. 2018K262).

ORCID iDs

Paolo Facchi https://orcid.org/0000-0001-9152-6515
Saverio Pascazio https://orcid.org/0000-0002-7214-5685
Kazuya Yuasa https://orcid.org/0000-0001-5314-2780

References

[1] Nielsen M A and Chuang I L 2000 *Quantum Computation and Quantum Information* (Cambridge: Cambridge University Press)
[2] Bengtsson I and Życzkowski K 2009 *Geometry of Quantum States: an Introduction to Quantum Entanglement* (Cambridge: Cambridge University Press)
[3] Wootters W K 2001 Entanglement of formation and concurrence *Quantum Inf. Comput.* **1** 27
[4] Amico L, Fazio R, Osterloh A and Vedral V 2008 Entanglement in many-body systems *Rev. Mod. Phys.* **80** 517
[5] Horodecki R, Horodecki P, Horodecki M and Horodecki K 2009 Quantum entanglement *Rev. Mod. Phys.* **81** 865
[6] Lubkin E 1978 Entropy of an *n*-system from its correlation with a *k*-reservoir *J. Math. Phys.* **19** 1028
[7] Page D N 1993 Average entropy of a subsystem *Phys. Rev. Lett.* **71** 1291
[8] Foong S K and Kanno S 1994 Proof of Page's conjecture on the average entropy of a subsystem *Phys. Rev. Lett.* **72** 1148
[9] Sánchez-Ruiz J 1995 Simple proof of Page's conjecture on the average entropy of a subsystem *Phys. Rev.* E **52** 5653
[10] Sen S 1996 Average entropy of a quantum subsystem *Phys. Rev. Lett.* **77** 1

[11] Giraud O 2007 Purity distribution for bipartite random pure states *J. Phys. A: Math. Theor.* **40** F1053
[12] Hayden P, Leung D W and Winter A 2006 Aspects of generic entanglement *Commun. Math. Phys.* **265** 95
[13] Facchi P, Marzolino U, Parisi G, Pascazio S and Scardicchio A 2008 Phase transitions of bipartite entanglement *Phys. Rev. Lett.* **101** 050502
[14] De Pasquale A, Facchi P, Parisi G, Pascazio S and Scardicchio A 2010 Phase transitions and metastability in the distribution of the bipartite entanglement of a large quantum system *Phys. Rev.* A **81** 052324
[15] De Pasquale A, Facchi P, Giovannetti V, Parisi G, Pascazio S and Scardicchio A 2012 Statistical distribution of the local purity in a large quantum system *J. Phys. A: Math. Theor.* **45** 015308
[16] Nadal C, Majumdar S N and Vergassola M 2010 Phase transitions in the distribution of bipartite entanglement of a random pure state *Phys. Rev. Lett.* **104** 110501
[17] Nadal C, Majumdar S N and Vergassola M 2011 Statistical distribution of quantum entanglement for a random bipartite state *J. Stat. Phys.* **142** 403
[18] Facchi P, Florio G, Parisi G, Pascazio S and Yuasa K 2013 Entropy-driven phase transitions of entanglement *Phys. Rev.* A **87** 052324
[19] Dyson F J 1962 Statistical theory of energy levels of complex systems II *J. Math. Phys.* **3** 157
[20] Forrester P J 2010 *Log-Gases and Random Matrices* (Princeton, NJ: Princeton University Press)
[21] Cunden F D, Facchi P, Florio G and Pascazio S 2013 Typical entanglement *Eur. Phys. J. Plus* **128** 48
[22] Cunden F D, Facchi P and Florio G 2013 Polarized ensembles of random pure states *J. Phys. A: Math. Theor.* **46** 315306
[23] Cunden F D, Facchi P and Vivo P 2016 A shortcut through the Coulomb gas method for spectral linear statistics on random matrices *J. Phys. A: Math. Theor.* **49** 135202
[24] Cunden F D, Facchi P, Ligabò M and Vivo P 2017 Universality of the third-order phase transition in the constrained Coulomb gas *J. Stat. Mech.* 053303
[25] Kosterlitz J M, Thouless D J and Jones R C 1976 Spherical model of a spin-glass *Phys. Rev. Lett.* **36** 1217
[26] Jones R C, Kosterlitz J M and Thouless D J 1978 The eigenvalue spectrum of a large symmetric random matrix with a finite mean *J. Phys. A: Math. Gen.* **11** L45
[27] Gross D J and Witten E 1980 Possible third order phase transition in the large-*N* lattice gauge theory *Phys. Rev.* D **21** 446
[28] 't Hooft G 1974 A planar diagram theory for strong interactions *Nucl. Phys.* B **72** 461
[29] Brezin E, Itzykson C, Parisi G and Zuber J B 1978 Planar diagrams *Commun. Math. Phys.* **59** 35
[30] Majumdar S N and Schehr G 2014 Top eigenvalue of a random matrix: large deviations and third order phase transition *J. Stat. Mech.* P01012
[31] Cunden F D, Facchi P, Ligabò M and Vivo P 2018 Universality of the weak pushed-to-pulled transition in systems with repulsive interactions *J. Phys. A: Math. Theor.* **51** 35LT01
[32] Lloyd S and Pagels H 1988 Complexity as thermodynamic depth *Ann. Phys., NY* **188** 186
[33] Życzkowski K and Sommers H-J 2001 Induced measures in the space of mixed quantum states *J. Phys. A: Math. Gen.* **34** 7111
[34] Itzykson C and Zuber J-B 1980 The planar approximation. II *J. Math. Phys.* **21** 411
[35] Marčenko V A and Pastur L A 1967 Distribution of eigenvalues for some sets of random matrices *Math. USSR Sb.* **1** 457
[36] Tricomi F G 1957 *Integral Equations* (Cambridge: Cambridge University Press)
[37] Facchi P, Florio G, Parisi G and Pascazio S 2008 Maximally multipartite entangled states *Phys. Rev.* A **77** 060304
[38] Facchi P, Florio G, Marzolino U, Parisi G and Pascazio S 2010 Classical statistical mechanics approach to multipartite entanglement *J. Phys. A: Math. Theor.* **43** 225303
[39] Goyeneche D, Alsina D, Latorre J I, Riera A and Życzkowski K 2015 Absolutely maximally entangled states, combinatorial designs and multi-unitary matrices *Phys. Rev.* A **92** 032316
[40] Goyeneche D and Życzkowski K 2014 Genuinely multipartite entangled states and orthogonal arrays *Phys. Rev.* A **90** 022316
[41] Goyeneche D, Bielawski J and Życzkowski K 2016 Multipartite entanglement in heterogeneous systems *Phys. Rev.* A **94** 012346
[42] Goyeneche D, Raissi Z, Di Martino S and Życzkowski K 2018 Entanglement and quantum combinatorial designs *Phys. Rev.* A **97** 062326

[43] Gour G and Wallach N R 2010 All maximally entangled four-qubit states *J. Math. Phys.* **51** 112201
[44] Huber F, Gühne O and Siewert J 2017 Absolutely maximally entangled states of seven qubits do not exist *Phys. Rev. Lett.* **118** 200502
[45] Facchi P, Florio G, Marzolino U, Parisi G and Pascazio S 2010 Multipartite entanglement and frustration *New J. Phys.* **12** 025015
[46] Zhang J, Adesso G, Xie C and Peng K 2009 Quantum teamwork for unconditional multiparty communication *Phys. Rev. Lett.* **103** 070501